SCIENCE CHINA
Information Sciences

• RESEARCH PAPER •

November 2018, Vol. 61 112205:1–112205:16
https://doi.org/10.1007/s11432-017-9309-3

Distributed sensor fault diagnosis for a formation system with unknown constant time delays

Donghua ZHOU[1,2*], Liguo QIN[2], Xiao HE[2], Rui YAN[2] & Ruiliang DENG[2]

[1]*College of Electrical Engineering and Automation, Shandong University of Science and Technology, Qingdao* 266590*, China;*
[2]*Department of Automation, TNList, Tsinghua University, Beijing* 100084*, China*

Received 26 June 2017/Accepted 30 November 2017/Published online 10 October 2018

Abstract In this paper, a distributed velocity sensor fault diagnosis scheme is presented for a formation of a second-order multi-agent system with unknown constant communication time delays. An existing distributed proportion-derivation (DPD) formation control law is adopted and a delay-independent condition is proposed to guarantee the asymptotical formation stability of the formation system based on the Nyquist stability criterion. Then a distributed fault diagnosis scheme is developed. In each agent, a distributed fault detection residual generator (DFDRG) and a bank of distributed fault isolation residual generators (DFIRGs) are designed based on the closed-loop model of the whole system. Each DFIRG is built up on the basis of a reduced-order unknown input observer (UIO) which is robust to the fault of one neighboring agent. According to the robust relationship between DFIRGs and faults, distributed fault isolation can be achieved. Conditions are presented to guarantee that each agent is able to diagnose faults of itself and its neighbors despite the disturbance of time delays. Finally, outdoor experimental results illustrate the effectiveness of the proposed schemes.

Keywords formation systems, distributed fault diagnosis, sensor faults, time delays, quadrotor unmanned helicopters

Citation Zhou D H, Qin L G, He X, et al. Distributed sensor fault diagnosis for a formation system with unknown constant time delays. Sci China Inf Sci, 2018, 61(11): 112205, https://doi.org/10.1007/s11432-017-9309-3

1 Introduction

In recent years, distributed formation control has attracted a great deal of attention in many fields such as rescue, surveillance, and space exploration. Compared with single dynamic systems, the merits of formation systems include reducing cost, increasing robustness, enhancing efficiency, and providing redundancy [1]. A lot of research has been published on distributed formation control [2–10]. A detailed survey of distributed formation control for multi-agent systems has been conducted in [1].

In practice, communication time delays are ubiquitous in formation systems because information transmission between agents is always influenced by environment disturbances, communication congestions, and limited transmission bandwidth [11, 12]. Moreover, communication time delays will inevitably deteriorate the stability of formation systems. Hence, it is important to study the formation stability of multi-agent systems with time delays. Current approaches on consensus or stability of distributed formations with time delays can be mainly categorized into time domain methods and frequency domain methods. In time domain methods, Lyapunov functions are always used to analyze consensus or

* Corresponding author (email: zdh@mail.tsinghua.edu.cn)

formation stability of multi-agent systems [13–15]. Nonetheless, results derived based on time domain methods are conservative owning to the conservation of Lyapunov functions. Different from time domain methods, frequency domain methods are able to reduce the conservation of results. In frequency domain methods, consensus or formation stability conditions are obtained by analyzing the poles of the closed-loop transfer function of a multi-agent system through techniques such as Nyquist stability criterion and τ-decomposition. Although some research has been carried out on consensus or formation stability of first-order multi-agent systems with time delays by using frequency domain methods [16–19], that of second-order multi-agent systems with time delays has not yet been closely investigated. In the paper, the formation problem for a network of second-order multi-agent system with constant communication time delays is considered. Under a distributed proportion-derivation (DPD) control law presented in [20], a delay-independent condition on the asymptotical formation stability is proposed based on the Nyquist stability criterion.

In the application of formation systems, the successful execution of tasks requires that the formation can be maintained and each agent operates in a fault-free manner [21]. However, there are only a handful of studies reported to date that consider fault diagnosis for formation systems. In [22], current fault diagnosis schemes for formation systems were surveyed and were divided into two types, namely, centralized schemes [23] and distributed schemes [24–27]. In a centralized scheme, the fault diagnosis algorithm operates in a single agent. The agent is able to diagnose faults in the whole system by using information transmitted from all the other agents. It can be seen that the centralized fault diagnosis scheme suffers from a single point of failure and less scalability [21]. In a distributed fault diagnosis scheme, the fault diagnosis algorithm is implemented in all agents. Each agent is able to diagnose faults in itself and its neighbors by using the information of itself and its neighbors. Compared with centralized schemes, distributed fault diagnosis ones have shown promising advantages in terms of robustness, scalability, and reliability [21].

However, up to now, there have been very few studies carried out on distributed fault diagnosis schemes for formation systems. Existing distributed fault diagnosis schemes can be divided into two categories, i.e., local-model based schemes and global-model based schemes. The design of a local-model based scheme in each agent requires both the model of the agent and models of neighbors of the agent, while that of a global-model based scheme requires the model of the whole system. Admittedly, a local-model based scheme has less computation loads than a global-model based one, but the communication load of a local-model based scheme is higher than that of a global-model based scheme. More concretely, in each agent, a global-model based fault diagnosis scheme only needs output information of neighbors. However, a local-model based scheme in each agent also requires the input besides the output of neighbors [26,27]. Furthermore, when there are communication time delays between agents, diagnosis results of local-model based schemes will be impacted by both the delayed input and the delayed output of neighbors. Hence, in case of time delays, it is more suitable to adopt a global-model based fault diagnosis scheme where diagnosis results are not disturbed by the delayed input of neighbors.

In [21], a distributed fault detection scheme was proposed for a formation of mobile robots based on a Kalman filter which was developed on the basis of the model of the whole system. In [28], an observer-based distributed fault diagnosis strategy for a team of first-order robots was designed. The distributed observer was developed based on the model of the whole system. A distributed fault diagnosis scheme for a second-order multi-agent system with actuator faults was presented in [29]. In each agent, a bank of distributed full-order unknown input observers (UIOs) were designed based on the closed-loop model of the entire system to achieve distributed fault isolation. Similar results can also be found in [30] where communication faults between agents were also considered. In [31], a distributed global-model based fault diagnosis scheme was developed for a discrete-time second-order multi-agent system with actuator faults and Gaussian white noises. A bank of distributed optimal robust observers were designed in each agent to achieve distributed fault isolation. In [32], a reduced-order UIO based distributed fault isolation scheme was developed for a general linear multi-agent system with actuator faults and disturbances based on the closed-loop model of the whole system. Compared with full-order UIO-based schemes in [29–31], the reduced-order UIO-based schemes in [32] has less computation loads.

Most of the aforementioned studies on distributed fault diagnosis for formation systems are carried out without considering communication time delays between agents. So far, there have been seldom attempts to design distributed fault diagnosis schemes for formation systems with time delays. Communication time delays increase the difficulties of designing fault diagnosis schemes and disturb fault diagnosis results because time delays introduce nonlinear dynamics into the model of a formation system. Moreover, most of the current distributed fault diagnosis schemes are illustrated only by simulations and lack practical experimental verification. To the knowledge of the authors, so far, very few outdoor experimental results on the distributed fault diagnosis for formation systems have been published. Motivated by these considerations, in the paper, a distributed sensor fault diagnosis scheme is proposed for a formation of a second-order multi-agent system subject to unknown constant communication time delays. In each agent, a distributed fault diagnosis scheme consisting of a distributed fault detection unit and a bank of distributed fault isolation units is developed. In the distributed fault detection unit, a distributed fault detection residual generator (DFDRG) is developed based on the model of the whole system. In each distributed fault isolation unit, a distributed fault isolation residual generator (DFIRG) is built up based on a reduced-order UIO and the closed-loop model of the system. Each DFIRG is robust to the fault of one neighboring agent. Moreover, each agent updates the states of its DFDRG and DFIRGs by using the output of itself and the relative output between itself and its neighbors. It is obtained that despite time delays, the proposed scheme is able to guarantee the accurate fault diagnosis results when sensor faults are constants or have a period equal to the time delay.

The novel contributions of the paper are summarized as follows. (1) A delay-independent condition on the formation stability of a second-order multi-agent system with constant time delays is proposed. (2) New DFIRGs are proposed based on the reduced-order UIOs for formation systems with constant time delays. (3) Conditions on the existence of the DFDRGs and DFIRGs are provided. (4) An outdoor experiment is carried out to illustrate the effectiveness of the DPD control law and the distributed fault diagnosis scheme based on a formation platform consisting of three quadrotors.

The rest of the paper is organized as follows. In Section 2, some preliminaries are presented and the problem statement is given. The distributed fault diagnosis scheme is proposed in Section 3. Experimental results are presented in Section 4. Finally, in Section 5, the conclusion is given.

Notation. In the paper, $\mathbb{R}$ represents the set of real numbers. $\mathbb{R}^n$ denotes the set of vectors with n dimensions. $\mathbf{0}_N$ is a zero matrix with $N \times N$ dimensions. $\mathbf{0}_{m\times n}$ is a zero matrix with $m \times n$ dimensions. $\boldsymbol{I}_N$ is the identity matrix with N dimensions. $\mathbf{1}_N$ represents an N dimension vector with all elements being 1. $\|\boldsymbol{r}\|$ denotes the Euclid norm of the vector $\boldsymbol{r}$. $\boldsymbol{W}^{\mathrm{T}}$ is the transposition of the matrix $\boldsymbol{W}$. $\boldsymbol{W}^{\dagger}$ stands for the Moore-Penrose pseudoinverse of the matrix $\boldsymbol{W}$. null($\boldsymbol{W}$) is the basis matrix of the null space of the matrix $\boldsymbol{W}$. $\rho\{\boldsymbol{W}\}$ stands for the set of eigenvalues of the matrix $\boldsymbol{W}$. diag$\{\lambda_1, \lambda_2, \ldots, \lambda_N\}$ represents the diagonal matrix where elements in the diagonal place are $\lambda_1, \lambda_2, \ldots, \lambda_N$. The symbol $\otimes$ represents the Kronecker product. $\bigwedge$ stands for the logic and operation. $\mathcal{A}\bigcup\mathcal{B}$ is the union of sets $\mathcal{A}$ and $\mathcal{B}$. $\mathcal{A}\backslash\mathcal{B}$ denotes the relative complement of set $\mathcal{B}$ in set $\mathcal{A}$.

2 Problem statement and preliminaries

2.1 Some preliminaries

Let $\mathcal{G} = \{\mathcal{V}, \mathcal{E}\}$ denote the communication topology of the multi-agent system, where $\mathcal{V} = \{1, \ldots, N\}$ represents the set of agents and $\mathcal{E} \subseteq \mathcal{V} \times \mathcal{V}$ represents the set of edges between agents. $(i, j) \in \mathcal{E}$ denotes an edge from agent i to agent j which means that agent j can obtain information from agent i, and agent i is called a neighbor of agent j. Define $\mathcal{N}_i \subseteq \mathcal{V}$ as the set of neighbors of agent i. $|\mathcal{N}_i|$ is the cardinality of the set $\mathcal{N}_i$. $\bar{\mathcal{N}}_i = \mathcal{N}_i \bigcup \{i\}$ represents the set including the ith agent and the neighbors of the ith agent. Let matrix $\boldsymbol{A}_g = [a_{ij}]$ be the adjacent matrix of $\mathcal{G}$, where $a_{ii} = 0$, $a_{ji} > 0$ if and only if $(i, j) \in \mathcal{E}$ and $a_{ji} = 0$ if $(i, j) \notin \mathcal{E}$ for $i, j = 1, 2, \ldots, N$. Let the diagonal matrix $\boldsymbol{D}_g = [d_{ij}]$ be the degree matrix of $\mathcal{G}$, where $d_{ii} = \sum_{j=0}^{N} a_{ij}$, and $d_{ij} = 0$ if $i \neq j$, for $i, j = 1, 2, \ldots, N$. The Laplacian matrix $\boldsymbol{L}_g$ of $\mathcal{G}$ is defined as $\boldsymbol{L}_g = \boldsymbol{D}_g - \boldsymbol{A}_g$. Some properties of the Kronecker product are $(\boldsymbol{A} \otimes \boldsymbol{B})(\boldsymbol{C} \otimes \boldsymbol{D}) = (\boldsymbol{AC}) \otimes (\boldsymbol{BD})$,

$(\boldsymbol{A}+\boldsymbol{B})\otimes\boldsymbol{C}=\boldsymbol{A}\otimes\boldsymbol{C}+\boldsymbol{B}\otimes\boldsymbol{C}$, and $\boldsymbol{A}\otimes(\boldsymbol{B}+\boldsymbol{C})=\boldsymbol{A}\otimes\boldsymbol{B}+\boldsymbol{A}\otimes\boldsymbol{C}$.

2.2 Problem statement

Consider a multi-agent system consisting of N second-order integrators and the model of the ith agent is

$$\begin{cases}\dot{\xi}_i(t)=\zeta_i(t),\\ \dot{\zeta}_i(t)=u_i(t),\\ y_i^{\xi}(t)=\xi_i(t),\\ y_i^{\zeta}(t)=\zeta_i(t)+f_i(t),\end{cases}\tag{1}$$

where $\xi_i\in\mathbb{R}$ and $\zeta_i\in\mathbb{R}$ represent the displacement and velocity of the ith agent, respectively. $u_i\in\mathbb{R}$ is the input of the ith agent. $y_i^{\xi}\in\mathbb{R}$ and $y_i^{\zeta}\in\mathbb{R}$ denote the sensor measurement of displacement and velocity of the ith agent, respectively. $f_i\in\mathbb{R}$ is the velocity sensor fault of the ith agent. The dimension of the second-order integrator considered in the paper is one, and results of agents with higher dimensions can be simply extended from results here.

The formula of $f_i(t)$ is

$$f_i(t)=\begin{cases}0, & t<T_i,\\ \chi_i(t-T_i), & t\geqslant T_i,\end{cases}\tag{2}$$

where $T_i\in\mathbb{R}$ is the time instant when fault occurs in the ith agent. $\chi_i(t)\in\mathbb{R}$ is the amplitude of the fault in the ith agent at time instant t.

Let $r(t)\in\mathbb{R}$ be the given trajectory of the multi-agent system. Define $\boldsymbol{d}=[d_1,d_2,\ldots,d_N]^{\mathrm{T}}$ as the formation vector of the multi-agent system, where $d_i\in\mathbb{R}$ is the relative distance between the ith agent and the virtual leader. Some assumptions are required in the paper.

Assumption 1. The communication topology of the system is undirected and connected.

Remark 1. Under Assumption 1, according to [3], the Laplacian matrix $\boldsymbol{L}_g$ is symmetrical and the eigenvalues of $\boldsymbol{L}_g$ satisfy $0=\lambda_1<\lambda_2\leqslant\cdots\leqslant\lambda_N$, where $\lambda_i\in\rho\{\boldsymbol{L}_g\}$, $i\in\{1,2,\ldots,N\}$.

Assumption 2. The first-order and second-order derivatives of the given trajectory exist.

Define the tracking error of the ith agent as $e_i(t)=r(t)+d_i-\xi_i(t)$. The definition of the asymptotical formation stability is described as follows.

Definition 1 (Asymptotical formation stability [33])**.** Given a multi-agent system with communication topology $\mathcal{G}$ and agents described as (1), the formation is said to be asymptotically stable if for any initial conditions, $\lim_{t\to\infty}e_i(t)=0$ holds, $i=1,2,\ldots,N$.

According to Assumption 2 and [20], the following DPD controller can be designed for the ith agent when there is no fault.

$$\begin{aligned}u_i(t)=&\,k_1[r(t)+d_i-y_i^{\xi}(t)]+k_3[\dot{r}(t)-y_i^{\zeta}(t)]+k_2\sum_{j\in\mathcal{N}_i}a_{ij}\left[y_j^{\xi}(t-\tau)-d_j-y_i^{\xi}(t-\tau)+d_i\right]\\&+k_4\sum_{j\in\mathcal{N}_i}a_{ij}\left[y_j^{\zeta}(t-\tau)-y_i^{\zeta}(t-\tau)\right]+\ddot{r}(t),\end{aligned}\tag{3}$$

where $i=1,2,\ldots,N$. $k_1>0$, $k_2>0$, $k_3>0$, and $k_4>0$ are parameters to be designed. $\tau\geqslant0$ is the constant communication time delay. It is assumed that $y_i^{\xi}(t-\tau)=0$ and $y_i^{\zeta}(t-\tau)=0$ hold when $t\leqslant\tau$, $i=1,2,\ldots,N$.

Note that in [20], the asymptotical formation stability conditions are presented without considering time delays. The following theorem presents a delay-independent condition on the asymptotical stability of the formation system with time delays.

Lemma 1. Given a multi-agent system with the communication topology $\mathcal{G}$ and agents described as (1), under the DPD control law (3), when there is no sensor fault, the asymptotical formation stability can be achieved for any finite time delay τ if $k_1>k_2\lambda_N$ and $k_3^2-2k_1-k_4^2\lambda_N^2>0$ hold.

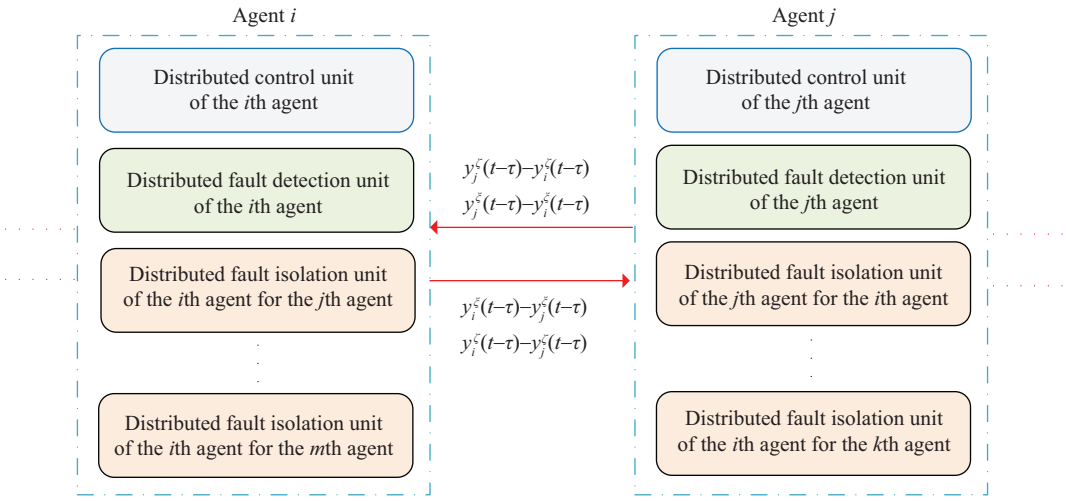

Figure 1 (Color online) The framework of the distributed fault diagnosis scheme for the formation system with time delays.

Proof. Please refer to Appendix A.

The objective of the paper is to design a distributed fault diagnosis scheme for a multi-agent system with constant time delays such that each agent in the system is able to diagnosis sensor faults of itself and its neighbors. Assume that there is only one velocity sensor fault in the multi-agent system at one moment. In order to reduce communication loads and decrease the influence of the time delays, a global-model based distributed fault diagnosis scheme is designed. The framework of the distributed fault diagnosis scheme for the multi-agent system is described in Figure 1.

In each agent, the distributed fault diagnosis scheme consists of a distributed fault detection unit and a bank of the distributed fault isolate units. The distributed fault detection unit includes a DFDRG which is developed based on a Luenberger observer and the closed-loop model of the entire system. According to the results of the distributed fault detection unit, each agent is able to detect faults of itself and its neighbors. In each distributed fault isolation unit, a DFIRG is a reduced-order UIO which is designed according to the closed-loop model of the entire system. The residual of each DFIRG is robust to the fault of one neighboring agent and sensitive to faults of other neighboring agents. For instance, the residual in the distributed fault isolation unit of the ith agent for the jth agent is robust to the fault of the jth agent and is sensitive to faults of other agents. According to the relationship of sensitivity (or robustness) between residuals and faults, each agent is able to isolate faults of its neighbors by combining the residuals of DFIRGs in the agent.

Note that in each agent, all information used to update states of the DFDRG and DFIRGs is the output of the agent and relative output between the agent and the neighbors of the agent, which is same as the information used in the DPD control law. It is obvious that this global-model based scheme has very few communication loads, which is suitable for the case when time delays exist.

3 Distributed fault diagnosis

In this section, a global-model based distributed fault diagnosis scheme for a multi-agent system with sensor faults and time delays is proposed. Firstly, the closed-loop model of the whole system is obtained. Then based on the model, the distributed fault detection and isolation schemes are designed.

According to (1) and (3), the closed-loop model of the ith agent is

$$\begin{cases} \dot{\xi}_i(t) = \zeta_i(t), \\ \dot{\zeta}_i(t) = -k_1\xi_i(t) - k_3\zeta_i(t) + k_2\sum\limits_{j\in\mathcal{N}_i} a_{ij}[\xi_j(t-\tau) - \xi_i(t-\tau)] + v_i(t) - k_3 f_i(t) \\ \qquad\quad + k_4\sum\limits_{j\in\mathcal{N}_i} a_{ij}[\zeta_j(t-\tau) - \zeta_i(t-\tau)] + k_4\sum\limits_{j\in\mathcal{N}_i} a_{ij}[f_j(t-\tau) - f_i(t-\tau)], \end{cases} \tag{4}$$

where $\xi_i(t-\tau) = 0$, $\zeta_i(t-\tau) = 0$, and $f_i(t-\tau) = 0$ hold when $t \leqslant \tau$, $i = 1, 2, \ldots, N$. $v_i(t) \in \mathbb{R}$ is the input of the closed-loop model of the ith agent and the formula of $v_i(t)$ is

$$v_i(t) = k_1[r(t) + d_i] + k_2\sum_{j\in\mathcal{N}_i} a_{ij}[d_i - d_j] + k_3\dot{r}(t) + \ddot{r}(t). \tag{5}$$

Let $\boldsymbol{x} = [\xi_1, \xi_2, \ldots, \xi_N, \zeta_1, \zeta_2, .., \zeta_N]^{\mathrm{T}}$, $\boldsymbol{v} = [v_1, v_2, \ldots, v_N]^{\mathrm{T}}$, $\boldsymbol{f} = [f_1, f_2, \ldots, f_N]^{\mathrm{T}}$, and $\boldsymbol{y}_i(t) = [y_i^{\xi}(t), y_{i_1}^{\xi}(t-\tau) - y_i^{\xi}(t-\tau), \ldots, y_{i_{|\mathcal{N}_i|}}^{\xi}(t-\tau) - y_i^{\xi}(t-\tau), y_i^{\zeta}(t), y_{i_1}^{\zeta}(t-\tau) - y_i^{\zeta}(t-\tau), \ldots, y_{i_{|\mathcal{N}_i|}}^{\zeta}(t-\tau) - y_i^{\zeta}(t-\tau)]^{\mathrm{T}}$. Note that $\boldsymbol{y}_i(t)$ only includes the sensor measurement of the ith agent and the relative output between the ith agent and the neighbors of the ith agent.

Then the closed-loop dynamic model of the multi-agent system is

$$\begin{cases} \dot{\boldsymbol{x}}(t) = \boldsymbol{A}_1\boldsymbol{x}(t) + \boldsymbol{A}_2\boldsymbol{x}(t-\tau) + \boldsymbol{B}\boldsymbol{v}(t) + \boldsymbol{E}_1\boldsymbol{f}(t) + \boldsymbol{E}_2\boldsymbol{f}(t-\tau), \\ \boldsymbol{y}_i(t) = \boldsymbol{C}_{i,1}\boldsymbol{x}(t) + \boldsymbol{C}_{i,2}\boldsymbol{x}(t-\tau) + \boldsymbol{\Gamma}_{i,1}\boldsymbol{f}(t) + \boldsymbol{\Gamma}_{i,2}\boldsymbol{f}(t-\tau), \end{cases} \tag{6}$$

where

$$\boldsymbol{A}_1 = \begin{bmatrix} \boldsymbol{0}_N & \boldsymbol{I}_N \\ -k_1\boldsymbol{I}_N & -k_3\boldsymbol{I}_N \end{bmatrix},\ \boldsymbol{A}_2 = \begin{bmatrix} \boldsymbol{0}_N & \boldsymbol{0}_N \\ -k_2\boldsymbol{L}_g & -k_4\boldsymbol{L}_g \end{bmatrix},\ \boldsymbol{B} = \begin{bmatrix} \boldsymbol{0}_N \\ \boldsymbol{I}_N \end{bmatrix},\ \boldsymbol{E}_1 = \begin{bmatrix} \boldsymbol{0}_N \\ -k_3\boldsymbol{I}_N \end{bmatrix},\ \boldsymbol{E}_2 = \begin{bmatrix} \boldsymbol{0}_N \\ -k_4\boldsymbol{L}_g \end{bmatrix},$$

$$\boldsymbol{C}_{i,1} = \begin{bmatrix} \boldsymbol{i}_i^{\mathrm{T}} \\ \boldsymbol{0}_{|\mathcal{N}_i|\times 2N} \\ \boldsymbol{i}_{i+N}^{\mathrm{T}} \\ \boldsymbol{0}_{|\mathcal{N}_i|\times 2N} \end{bmatrix},\ \boldsymbol{C}_{i,2} = \begin{bmatrix} \boldsymbol{0}_{1\times 2N} \\ \boldsymbol{i}_{i_1}^{\mathrm{T}} - \boldsymbol{i}_i^{\mathrm{T}} \\ \vdots \\ \boldsymbol{i}_{i_{|\mathcal{N}_i|}}^{\mathrm{T}} - \boldsymbol{i}_i^{\mathrm{T}} \\ \boldsymbol{0}_{1\times 2N} \\ \boldsymbol{i}_{i_1+N}^{\mathrm{T}} - \boldsymbol{i}_{i+N}^{\mathrm{T}} \\ \vdots \\ \boldsymbol{i}_{i_{|\mathcal{N}_i|}+N}^{\mathrm{T}} - \boldsymbol{i}_{i+N}^{\mathrm{T}} \end{bmatrix},\ \boldsymbol{\Gamma}_{i,1} = \begin{bmatrix} \boldsymbol{0}_{(|\mathcal{N}_i|+1)\times N} \\ \hat{\boldsymbol{i}}_i^{\mathrm{T}} \\ \boldsymbol{0}_{|\mathcal{N}_i|\times N} \end{bmatrix},\ \boldsymbol{\Gamma}_{i,2} = \begin{bmatrix} \boldsymbol{0}_{(|\mathcal{N}_i|+1)\times N} \\ \boldsymbol{0}_{1\times N} \\ \hat{\boldsymbol{i}}_{i_1}^{\mathrm{T}} - \hat{\boldsymbol{i}}_i^{\mathrm{T}} \\ \vdots \\ \hat{\boldsymbol{i}}_{i_{|\mathcal{N}_i|}}^{\mathrm{T}} - \hat{\boldsymbol{i}}_i^{\mathrm{T}} \end{bmatrix}.$$

Moreover, $\boldsymbol{i}_k$ and $\hat{\boldsymbol{i}}_k$ are the kth columns of the identity matrix $\boldsymbol{I}_{2N}$ and $\boldsymbol{I}_N$, respectively. i_m is the index of the mth neighbors of the ith agent, $m = 1, 2, \ldots, |\mathcal{N}_i|$.

3.1 Distributed fault detection

In this subsection, a DFDRG is designed based on the closed-loop model of the system. Then a distributed fault detection logic is presented.

According to (6), the following DFDRG of the ith agent is developed based on the a Luenberger observer.

$$\begin{cases} \dot{\hat{\boldsymbol{x}}}_i^0(t) = (\boldsymbol{A}_1 + \boldsymbol{A}_2)\hat{\boldsymbol{x}}_i^0(t) + \boldsymbol{B}\boldsymbol{v}(t) + \boldsymbol{G}_i^0[\boldsymbol{y}_i(t) - (\boldsymbol{C}_{i,1} + \boldsymbol{C}_{i,1})\hat{\boldsymbol{x}}_i^0(t)], \\ \boldsymbol{r}_i^0(t) = \boldsymbol{y}_i(t) - (\boldsymbol{C}_{i,1} + \boldsymbol{C}_{i,2})\hat{\boldsymbol{x}}_i^0(t), \end{cases} \tag{7}$$

where $\hat{\boldsymbol{x}}_i^0 \in \mathbb{R}^{2N}$ is the states of the DFDRG in the ith agent. $\boldsymbol{r}_i^0 \in \mathbb{R}^{2|\mathcal{N}_i|+2}$ is the residual of the ith agent. $\boldsymbol{G}_i^0$ is the parameter to be designed.

Define the state estimation error of the DFDRG in the ith agent as $\boldsymbol{e}_i^0(t) = \boldsymbol{x}(t) - \hat{\boldsymbol{x}}_i^0(t)$. The following theorem presents the condition on the convergence of the state estimation error.

Theorem 1. When there is no sensor faults, given a multi-agent system with communication topology $\mathcal{G}$ and agents described as (6), there exists a matrix $\boldsymbol{G}_i^0$ such that the state estimation error $\boldsymbol{e}_i^0(t)$ approaches to zero asymptotically if the following two conditions are satisfied.

(1) The pair $(\boldsymbol{A}_1+\boldsymbol{A}_2, \boldsymbol{C}_{i,1}+\boldsymbol{C}_{i,2})$ is detectable.

(2) The closed-loop system (6) is asymptotically stable.

Proof. According to (6) and (7), it follows that

$$\dot{\boldsymbol{e}}_i^0(t) = \dot{\boldsymbol{x}}(t) - \dot{\hat{\boldsymbol{x}}}_i^0(t) = [(\boldsymbol{A}_1+\boldsymbol{A}_2) - \boldsymbol{G}_i^0(\boldsymbol{C}_{i,1}+\boldsymbol{C}_{i,2})]\boldsymbol{e}_i^0(t) + (\boldsymbol{A}_2 - \boldsymbol{G}_i^0\boldsymbol{C}_{i,2})[\boldsymbol{x}(t-\tau)-\boldsymbol{x}(t)].$$

Since $(\boldsymbol{A}_1+\boldsymbol{A}_2, \boldsymbol{C}_{i,1}+\boldsymbol{C}_{i,2})$ is detectable, there exists a matrix $\boldsymbol{G}_i^0$ such that $(\boldsymbol{A}_1+\boldsymbol{A}_2) - \boldsymbol{G}_i^0(\boldsymbol{C}_{i,1}+\boldsymbol{C}_{i,2})$ is stable. When there is no sensor fault, under the assumption that the system is stable, it follows that

$$\lim_{t\to\infty} \boldsymbol{x}(t) = \begin{bmatrix} r(t) \\ \dot{r}(t) \end{bmatrix} \otimes \boldsymbol{1}_N + \begin{bmatrix} \boldsymbol{d} \\ \boldsymbol{0}_{N\times 1} \end{bmatrix}. \tag{8}$$

Furthermore, it can be obtained that

$$\begin{aligned} &\lim_{t\to\infty} \boldsymbol{A}_2[\boldsymbol{x}(t-\tau)-\boldsymbol{x}(t)] = \left(\begin{bmatrix} 0 & 0 \\ -k_2 & -k_4 \end{bmatrix} \otimes \boldsymbol{L}_g\right)\left(\begin{bmatrix} r(t)-r(t-\tau) \\ \dot{r}(t)-\dot{r}(t-\tau) \end{bmatrix} \otimes \boldsymbol{1}_N\right) = \boldsymbol{0}_{2N\times 1}, \\ &\lim_{t\to\infty} \boldsymbol{C}_{i,2}[\boldsymbol{x}(t-\tau)-\boldsymbol{x}(t)] = \boldsymbol{0}_{(2|\mathcal{N}_i|+2)\times 1}. \end{aligned} \tag{9}$$

Then it is obvious that $\lim_{t\to\infty} \boldsymbol{e}_i^0(t) = \boldsymbol{0}_{(2|\mathcal{N}_i|+2)\times 1}$. This ends the proof.

Remark 2. Note that condition (2) in Theorem 1 is introduced to eliminate the disturbance of $\boldsymbol{x}(t-\tau)-\boldsymbol{x}(t)$. Without condition (2), $\boldsymbol{e}_i^0(t)$ may not converge to zeros even if there are no faults, which means that fault detection cannot be achieved. Moreover, condition (2) can be achieved according to Lemma 1.

Define $J_i^0(t) = \|\boldsymbol{r}_i^0(t)\|$ as the fault detection evaluation function of the ith agent. Let $J_{i,\mathrm{th}}^0 \in \mathbb{R}$ be the fault detection threshold of the ith agent. The fault detection logic of the ith agent is designed as Algorithm 1.

Algorithm 1 Fault detection logic of the ith agent

if $J_i^0(t) \geqslant J_{i,\mathrm{th}}^0$ **then**
  There is a fault in the system.
else
  There is no fault in the system.
end if

Remark 3. Note that it is very complex to set the value of $J_{i,\mathrm{th}}^0$ in practice. When there are no model uncertainties, disturbances, and noises, $J_{i,\mathrm{th}}^0$ can be set to be zero. Otherwise, the value of the threshold should be determined according to the fault detection rate, disturbances, uncertainties, and noises of the system. The interested readers may refer to [34, 35] for more approaches to design fault detection thresholds.

3.2 Distributed fault isolation

In this subsection, a distributed fault isolation scheme is proposed for the formation system. As described in Figure 1, in each agent, a bank of DFIRGs are designed based on reduced-order UIOs and the closed-loop model of the multi-agent system. The residual in each DFIRG of an agent is robust to one faulty neighbor and is sensitive to the other faulty neighbors. According to the relationship of sensitivity (or robustness) between residuals and faults, fault isolation logic is developed.

According to (6), given an agent i, provided that a sensor fault occurs in the kth agent, where $k \in \mathcal{N}_i$, the closed-loop dynamic model of the whole system is

$$\begin{cases} \dot{\boldsymbol{x}}_i^k(t) = \boldsymbol{A}_1\boldsymbol{x}_i^k(t) + \boldsymbol{A}_2\boldsymbol{x}_i^k(t-\tau) + \boldsymbol{B}\boldsymbol{v}(t) + \boldsymbol{E}_1^k f_k(t) + \boldsymbol{E}_2^k f_k(t-\tau), \\ \boldsymbol{y}_i(t) = \boldsymbol{C}_{i,1}\boldsymbol{x}(t) + \boldsymbol{C}_{i,2}\boldsymbol{x}(t-\tau) + \boldsymbol{\Gamma}_i^k f_k(t-\tau), \end{cases} \tag{10}$$

where $\boldsymbol{x}_i^k \in \mathbb{R}^{2N}$ is the state of of the whole system when there is a fault in the kth agent. $f_k(t-\tau) \in \mathbb{R}$ is the delayed fault of the kth agents. $\boldsymbol{E}_1^k$ is the kth column of $\boldsymbol{E}_1$ and represents the direction of $f_k(t)$ in the dynamic equation. $\boldsymbol{E}_2^k$ is the kth column of $\boldsymbol{E}_2$ and stands for the direction of $f_k(t-\tau)$ in the dynamic system. $\boldsymbol{\Gamma}_i^k$ is the kth column of $\boldsymbol{\Gamma}_{i,2}$ and denotes the direction of $f_k(t-\tau)$ in the output equation.

Remark 4. It can be seen from (10) that the dynamic equation and output equation are all disturbed by time delays, which increases the challenge of designing distributed fault diagnosis schemes. Moreover, the sensor fault of the kth agent disturbs both the dynamic equation and the output equation in (10), which makes the system more complicated.

In order to reduce computation loads of each agent, reduced-order UIOs are used to designed DFIRGs. According to [36], before designing reduced-order UIOs for (10), the output information which is directly disturbed by $f_k(t-\tau)$ should be removed firstly.

Define a matrix $\boldsymbol{U}_i^{k,0} = \{\text{null}[(\boldsymbol{\Gamma}_i^k)^{\mathrm{T}}]\}^{\mathrm{T}}$. It is obvious that $\boldsymbol{U}_i^{k,0}\boldsymbol{\Gamma}_i^k = 0$. Let $\boldsymbol{y}_i^k(t) = \boldsymbol{U}_i^{k,0}\boldsymbol{y}_i(t)$ be the new output. The new dynamic equation and output equation for the ith agent are obtained as follows.

$$\begin{cases} \dot{\boldsymbol{x}}_i^k(t) = \boldsymbol{A}_1\boldsymbol{x}_i^k(t) + \boldsymbol{A}_2\boldsymbol{x}_i^k(t-\tau) + \boldsymbol{B}\boldsymbol{v}(t) + \boldsymbol{E}_1^k f_k(t) + \boldsymbol{E}_2^k f_k(t-\tau), \\ \boldsymbol{y}_i^k(t) = \boldsymbol{C}_{i,1}^k\boldsymbol{x}(t) + \boldsymbol{C}_{i,2}^k\boldsymbol{x}(t-\tau), \end{cases} \tag{11}$$

where $\boldsymbol{y}_i^k \in \mathbb{R}^{2\mathcal{N}_i+1}$ is the new output which is not perturbed by the fault of the kth agent. Moreover, it follows that $\boldsymbol{C}_{i,1}^k = \boldsymbol{U}_i^{k,0}\boldsymbol{C}_{i,1}$ and $\boldsymbol{C}_{i,2}^k = \boldsymbol{U}_i^{k,0}\boldsymbol{C}_{i,2}$.

Remark 5. Owning to $f_k(t-\tau)$, the relative output $y_k^{\zeta}(t-\tau) - y_i^{\zeta}(t-\tau)$ should be deleted so that a decoupled residual generator can be designed. However, in the case of actuator fault, there is no need to delete any relative output information. The deletion of one output signal makes the design of diagnosis scheme for sensor faults more difficult than that for actuator faults.

According to [36], the following reduced-order UIO based DFIRG can be designed.

$$\begin{cases} \dot{\boldsymbol{z}}_i^k(t) = \boldsymbol{F}_i^k\boldsymbol{z}_i^k(t) + \boldsymbol{M}_i^k\boldsymbol{v}(t) + \boldsymbol{S}_i^k\boldsymbol{y}_i(t), \\ \boldsymbol{r}_i^k(t) = \boldsymbol{J}_i^k\boldsymbol{z}_i^k(t) + \boldsymbol{H}_i^k\boldsymbol{y}_i(t), \end{cases} \tag{12}$$

where $k \in \mathcal{N}_i$. $\boldsymbol{z}_i^k \in \mathbb{R}^{2N-1}$ and $\boldsymbol{r}_i^k(t) \in \mathbb{R}^{2\mathcal{N}_i}$ are the state and residual of DFIRG, respectively. $\boldsymbol{F}_i^k$, $\boldsymbol{M}_i^k$, $\boldsymbol{S}_i^k$, $\boldsymbol{J}_i^k$, and $\boldsymbol{H}_i^k$ are parameters to be designed.

Define the state estimation error of (12) as $\boldsymbol{e}_i^k(t) = \boldsymbol{N}_i^k\boldsymbol{x}_i^k(t) - \boldsymbol{z}_i^k(t)$, where $\boldsymbol{N}_i^k = [\text{null}((\boldsymbol{E}_i^k)^{\mathrm{T}})]^{\mathrm{T}}$ and $\boldsymbol{E}_i^k = \boldsymbol{E}_1^k + \boldsymbol{E}_2^k$. The following definition can be obtained.

Definition 2. The residual of the DFDRG (12) is said to be decoupled from a faulty agent k if $\boldsymbol{e}_i^k(t)$ approaches to zeros asymptotically regardless of the presence of $f_k(t)$ and $f_k(t-\tau)$.

The following theorem presents conditions to guarantee that $\boldsymbol{r}_i^k$ is decoupled from $f_k(t)$ and $f_k(t-\tau)$ and provides the design method of the parameters in (12).

Theorem 2. Given a system (10), let $\boldsymbol{E}_i^k = \boldsymbol{E}_1^k + \boldsymbol{E}_2^k$. Define $\boldsymbol{U}_i^{k,0} = \{\text{null}[(\boldsymbol{\Gamma}_i^k)^{\mathrm{T}}]\}^{\mathrm{T}}$, $\boldsymbol{C}_{i,1}^k = \boldsymbol{U}_i^{k,0}\boldsymbol{C}_{i,1}$, $\boldsymbol{C}_{i,2}^k = \boldsymbol{U}_i^{k,0}\boldsymbol{C}_{i,2}$, and $\boldsymbol{C}_i^k = \boldsymbol{C}_{i,1}^k + \boldsymbol{C}_{i,2}^k$. The residual $\boldsymbol{r}_i^k(t)$ in (12) is decoupled from the faulty agent k, $i = 1, 2, \ldots, N$, $k \in \mathcal{N}_i$, if the following conditions are satisfied.

(1) rank $(\boldsymbol{C}_i^k\boldsymbol{E}_i^k)$=rank $(\boldsymbol{E}_i^k)$;

(2) rank $\begin{bmatrix} {}^{s\boldsymbol{I}_{2N}-(\boldsymbol{A}_1+\boldsymbol{A}_2)} & \boldsymbol{E}_i^k \\ \boldsymbol{C}_i^k & \boldsymbol{0} \end{bmatrix}$=$2N + \text{rank}(\boldsymbol{E}_i^k)$, $\forall s \in C$, $Re(s) \geqslant 0$;

(3) The amplitude of the fault $\chi_k(t)$ in the kth agent is a constant or the period of $\chi_k(t)$ is equal to τ;

(4) The closed-loop system (6) is asymptotically stable.

Moreover, parameters of the DFIRG (12) can be designed as follows.

$$\begin{aligned} &\boldsymbol{N}_i^k = [\text{null}((\boldsymbol{E}_i^k)^{\mathrm{T}})]^{\mathrm{T}}, \quad (\boldsymbol{E}_i^k)^{\dagger} = [(\boldsymbol{E}_i^k)^{\mathrm{T}}(\boldsymbol{E}_i^k)]^{-1}(\boldsymbol{E}_i^k), \quad (\boldsymbol{N}_i^k)^{\dagger} = (\boldsymbol{N}_i^k)^{\mathrm{T}}[(\boldsymbol{N}_i^k)(\boldsymbol{N}_i^k)^{\mathrm{T}}]^{-1}, \\ &\boldsymbol{A}_{i,11}^k = \boldsymbol{N}_i^k(\boldsymbol{A}_1+\boldsymbol{A}_2)(\boldsymbol{N}_i^k)^{\dagger}, \quad \boldsymbol{A}_{i,12}^k = \boldsymbol{N}_i^k(\boldsymbol{A}_1+\boldsymbol{A}_2)\boldsymbol{E}_i^k, \\ &\boldsymbol{U}_i^{k,1} = (\boldsymbol{C}_i^k\boldsymbol{E}_i^k)^{\dagger} = [(\boldsymbol{C}_i^k\boldsymbol{E}_i^k)^{\mathrm{T}}(\boldsymbol{C}_i^k\boldsymbol{E}_i^k)]^{-1}(\boldsymbol{C}_i^k\boldsymbol{E}_i^k)^{\mathrm{T}}, \quad \boldsymbol{U}_i^{k,2} = [\text{null}((\boldsymbol{C}_i^k\boldsymbol{E}_i^k)^{\mathrm{T}})]^{\mathrm{T}}, \\ &\boldsymbol{F}_i^k = \boldsymbol{A}_{i,11}^k - \boldsymbol{A}_{i,12}^k\boldsymbol{U}_i^{k,1}\boldsymbol{C}_i^k(\boldsymbol{N}_i^k)^{\dagger} - \boldsymbol{G}_i^k\boldsymbol{U}_i^{k,2}\boldsymbol{C}_i^k(\boldsymbol{N}_i^k)^{\dagger}, \quad \boldsymbol{M}_i^k = \boldsymbol{N}_i^k\boldsymbol{B}, \\ &\boldsymbol{S}_i^k = \boldsymbol{A}_{i,12}^k\boldsymbol{U}_i^{k,1}\boldsymbol{U}_i^{k,0} + \boldsymbol{G}_i^k\boldsymbol{U}_i^{k,2}\boldsymbol{U}_i^{k,0}, \quad \boldsymbol{J}_i^k = -\boldsymbol{U}_i^{k,2}\boldsymbol{C}_i^k(\boldsymbol{N}_i^k)^{\dagger}, \quad \boldsymbol{H}_i^k = \boldsymbol{U}_i^{k,2}\boldsymbol{U}_i^{k,0}, \end{aligned} \tag{13}$$

where $\boldsymbol{G}_i^k$ is a matrix such that $\boldsymbol{F}_i^k = \boldsymbol{A}_{i,11}^k - \boldsymbol{A}_{i,12}^k \boldsymbol{U}_i^{k,1} \boldsymbol{C}_i^k (\boldsymbol{N}_i^k)^\dagger - \boldsymbol{G}_i^k \boldsymbol{U}_i^{k,2} \boldsymbol{C}_i^k (\boldsymbol{N}_i^k)^\dagger$ is stable.

Proof. Let $\Delta \boldsymbol{x}_i^k(t) = \boldsymbol{x}_i^k(t-\tau) - \boldsymbol{x}_i^k(t)$, $\Delta f_k(t) = f_k(t-\tau) - f_k(t)$. According to (11), it follows that

$$\begin{cases} \dot{\boldsymbol{x}}_i^k(t) = (\boldsymbol{A}_1 + \boldsymbol{A}_2)\boldsymbol{x}_i^k(t) + \boldsymbol{B}\boldsymbol{v}(t) + \boldsymbol{E}_i^k f_k(t) + \boldsymbol{A}_2 \Delta \boldsymbol{x}_i^k(t) + \boldsymbol{E}_2^k \Delta f_k(t), \\ \boldsymbol{y}_i^k(t) = \boldsymbol{C}_i^k \boldsymbol{x}(t) + \boldsymbol{C}_{i,2}^k \Delta \boldsymbol{x}_i^k(t). \end{cases} \tag{14}$$

Let $\boldsymbol{T}_i^k = [(\boldsymbol{N}_i^k)^{\mathrm{T}}\ ((\boldsymbol{E}_i^k)^\dagger)^{\mathrm{T}}]^{\mathrm{T}}$, $(\boldsymbol{T}_i^k)^{-1} = [(\boldsymbol{N}_i^k)^\dagger\ \boldsymbol{E}_i^k]$, $\tilde{\boldsymbol{x}}_i^k = \boldsymbol{T}_i^k \boldsymbol{x}_i^k = [(\tilde{\boldsymbol{x}}_{i,1}^k)^{\mathrm{T}}\ (\tilde{\boldsymbol{x}}_{i,2}^k)^{\mathrm{T}}]^{\mathrm{T}}$. By using $\boldsymbol{T}_i^k$, Eq. (14) can be transformed into the following equation.

$$\begin{cases} \begin{bmatrix} \dot{\tilde{\boldsymbol{x}}}_{i,1}^k(t) \\ \dot{\tilde{\boldsymbol{x}}}_{i,2}^k(t) \end{bmatrix} = \begin{bmatrix} \boldsymbol{A}_{i,11}^k & \boldsymbol{A}_{i,12}^k \\ \boldsymbol{A}_{i,21}^k & \boldsymbol{A}_{i,22}^k \end{bmatrix} \begin{bmatrix} \tilde{\boldsymbol{x}}_{i,1}^k(t) \\ \tilde{\boldsymbol{x}}_{i,2}^k(t) \end{bmatrix} + \begin{bmatrix} \boldsymbol{N}_i^k \boldsymbol{B} \\ (\boldsymbol{E}_i^k)^\dagger \boldsymbol{B} \end{bmatrix} \boldsymbol{v}(t) + \begin{bmatrix} \boldsymbol{0}_{(2N-1)\times 1} \\ 1 \end{bmatrix} f_k(t) \\ \qquad\qquad + \boldsymbol{T}_i^k \boldsymbol{A}_2 \Delta \boldsymbol{x}_i^k(t) + \boldsymbol{T}_i^k \boldsymbol{E}_2^k \Delta f_k(t), \\ \boldsymbol{y}_i^k(t) = \begin{bmatrix} \boldsymbol{C}_i^k (\boldsymbol{N}_i^k)^\dagger & \boldsymbol{C}_i^k \boldsymbol{E}_i^k \end{bmatrix} \begin{bmatrix} \tilde{\boldsymbol{x}}_{i,1}^k(t) \\ \tilde{\boldsymbol{x}}_{i,2}^k(t) \end{bmatrix} + \boldsymbol{C}_{i,2}^k \Delta \boldsymbol{x}_i^k(t). \end{cases} \tag{15}$$

where

$$\begin{bmatrix} \boldsymbol{A}_{i,11}^k & \boldsymbol{A}_{i,12}^k \\ \boldsymbol{A}_{i,21}^k & \boldsymbol{A}_{i,22}^k \end{bmatrix} = \boldsymbol{T}_i^k (\boldsymbol{A}_1 + \boldsymbol{A}_2)(\boldsymbol{T}_i^k)^{-1}. \tag{16}$$

According to the formula of $\boldsymbol{U}_i^{k,1}$ and $\boldsymbol{U}_i^{k,2}$, it follows that

$$\begin{cases} \boldsymbol{U}_i^{k,1} \boldsymbol{y}_i^k(t) = \boldsymbol{U}_i^{k,1} \boldsymbol{C}_i^k (\boldsymbol{N}_i^k)^\dagger \tilde{\boldsymbol{x}}_{i,1}^k(t) + \tilde{\boldsymbol{x}}_{i,2}^k(t) + \boldsymbol{U}_i^{k,1} \boldsymbol{C}_{i,2}^k \Delta \boldsymbol{x}_i^k(t), \\ \boldsymbol{U}_i^{k,2} \boldsymbol{y}_i^k(t) = \boldsymbol{U}_i^{k,2} \boldsymbol{C}_i^k (\boldsymbol{N}_i^k)^\dagger \tilde{\boldsymbol{x}}_{i,1}^k(t) + \boldsymbol{U}_i^{k,2} \boldsymbol{C}_{i,2}^k \Delta \boldsymbol{x}_i^k(t). \end{cases} \tag{17}$$

By combing the dynamic of $\tilde{\boldsymbol{x}}_{i,1}^k$ and (17), it follows that

$$\begin{cases} \dot{\tilde{\boldsymbol{x}}}_{i,1}^k(t) = [\boldsymbol{A}_{i,11}^k - \boldsymbol{A}_{i,12}^k \boldsymbol{U}_i^{k,1} \boldsymbol{C}_i^k (\boldsymbol{N}_i^k)^\dagger] \tilde{\boldsymbol{x}}_{i,1}^k(t) + \boldsymbol{A}_{i,12}^k \boldsymbol{U}_i^{k,1} \boldsymbol{y}_i^k(t) + \boldsymbol{N}_i^k \boldsymbol{B}\boldsymbol{v}(t) \\ \qquad\qquad + \boldsymbol{N}_i^k \boldsymbol{E}_2^k \Delta f_k(t) + (\boldsymbol{N}_i^k \boldsymbol{A}_2 - \boldsymbol{A}_{i,12}^k \boldsymbol{U}_i^{k,1} \boldsymbol{C}_{i,2}^k) \Delta \boldsymbol{x}_i^k(t), \\ \boldsymbol{U}_i^{k,2} \boldsymbol{y}_i^k(t) = \boldsymbol{U}_i^{k,2} \boldsymbol{C}_i^k (\boldsymbol{N}_i^k)^\dagger \tilde{\boldsymbol{x}}_{i,1}^k(t) + \boldsymbol{U}_i^{k,2} \boldsymbol{C}_{i,2}^k \Delta \boldsymbol{x}_i^k(t). \end{cases} \tag{18}$$

According to the second condition in Theorem 2 and [36], the pair $[\boldsymbol{A}_{i,11}^k - \boldsymbol{A}_{i,12}^k \boldsymbol{U}_i^{k,1} \boldsymbol{C}_i^k (\boldsymbol{N}_i^k)^\dagger$, $\boldsymbol{U}_i^{k,2} \boldsymbol{C}_i^k (\boldsymbol{N}_i^k)^\dagger]$ is detectable. Hence, there exists a matrix $\boldsymbol{G}_i^k$ such that the matrix $\boldsymbol{F}_i^k$ is stable. Then, parameters in (12) can be designed.

According to (12) and (18), it can be obtained that

$$\begin{cases} \dot{\boldsymbol{e}}_i^k(t) = \boldsymbol{F}_i^k \boldsymbol{e}_i^k(t) + (\boldsymbol{N}_i^k \boldsymbol{A}_2 - \boldsymbol{A}_{i,12}^k \boldsymbol{U}_i^{k,1} \boldsymbol{C}_{i,2}^k - \boldsymbol{G}_i^k \boldsymbol{U}_i^{k,2} \boldsymbol{C}_{i,2}^k) \Delta \boldsymbol{x}_i^k(t) + \boldsymbol{N}_i^k \boldsymbol{E}_2^k \Delta f_k(t), \\ \boldsymbol{r}_i^k(t) = -\boldsymbol{J}_i^k \boldsymbol{e}_i^k(t) + \boldsymbol{U}_i^{k,2} \boldsymbol{C}_{i,2}^k \Delta \boldsymbol{x}_i^k(t). \end{cases} \tag{19}$$

Since the system (6) is asymptotically stable, it follows that

$$\lim_{t\to\infty} \boldsymbol{x}_i^k(t) = \begin{bmatrix} r(t) \\ \dot{r}(t) \end{bmatrix} \otimes \boldsymbol{1}_N + \begin{bmatrix} \boldsymbol{d} \\ \boldsymbol{0}_{N\times 1} \end{bmatrix} + \boldsymbol{\Omega} \chi_k(t), \tag{20}$$

where $\boldsymbol{\Omega}$ is a matrix with appropriate dimensions.

If $\chi_k(t)$ is a constant or the period of $\chi_k(t)$ is equal to τ, it follows that

$$\begin{aligned} &\lim_{t\to\infty} \boldsymbol{A}_2[\boldsymbol{x}_i^k(t-\tau) - \boldsymbol{x}_i^k(t)] = \left(\begin{bmatrix} 0 & 0 \\ -k_2 & -k_4 \end{bmatrix} \otimes \boldsymbol{L}_g \right) \left(\begin{bmatrix} r(t) - r(t-\tau) \\ \dot{r}(t) - \dot{r}(t-\tau) \end{bmatrix} \otimes \boldsymbol{1}_N \right) = \boldsymbol{0}_{2N\times 1}, \\ &\lim_{t\to\infty} \boldsymbol{C}_{i,2}^k[\boldsymbol{x}_i^k(t-\tau) - \boldsymbol{x}_i^k(t)] = \boldsymbol{U}_i^{k,0} \boldsymbol{C}_{i,2}[\boldsymbol{x}_i^k(t-\tau) - \boldsymbol{x}_i^k(t)] = \boldsymbol{0}_{(2|\mathcal{N}_i|+1)\times 1}, \\ &\lim_{t\to\infty} \boldsymbol{N}_i^k \boldsymbol{E}_2^k \Delta f_k(t) = \boldsymbol{0}_{(2N-1)\times 1}. \end{aligned} \tag{21}$$

According to (19) and (21), when a sensor fault only occurs in the kth agent, it follows that $\lim_{t\to\infty} \boldsymbol{e}_i^k(t) = \boldsymbol{0}_{(2N-1)\times 1}$ and $\lim_{t\to\infty} \boldsymbol{r}_i^k(t) = \boldsymbol{0}_{2|\mathcal{N}_i|\times 1}$ hold. This ends the proof.

Remark 6. According to (14), in order to design a residual generator which is robust to $f_k(t)$, the residual must be decoupled from $f_k(t)$ and $\Delta f_k(t)$. However, owning to the deletion of $y_k^{\zeta}(t-\tau)-y_i^{\zeta}(t-\tau)$, condition (2) in Theorem 2 is hardly satisfied if $\boldsymbol{E}_i^k$ is replaced with $[\boldsymbol{E}_i^k\ \boldsymbol{E}_2^k]$. Therefore, condition (3) in Theorem 2 is introduced to eliminate the influence of $\Delta f_k(t)$. However, in case of an actuator fault, condition (3) is unnecessary, which means that there exists a residual generator decoupled from the actuator fault regardless of the amplitude of the fault.

Remark 7. Condition (4) in Theorem 2 is introduced to guarantee the equalities in (21). When the closed-loop model of the multi-agent system is not stable, equalities in (21) are not satisfied and $\lim_{t\to\infty}\boldsymbol{r}_i^k(t)$ is not equal to zero. In this case, $\boldsymbol{r}_i^k$ is not decoupled from the faulty agent k, which means that the distributed fault isolation cannot be achieved.

If a sensor fault occurs in the ith agent, the fault isolation can be achieved by using a simpler residual generator as (22) which is designed based on the open-loop model, the input information, and the output information of the ith agent.

$$\begin{cases}\dot{\hat{\boldsymbol{x}}}_i^i(t)=\boldsymbol{A}_i^i\hat{\boldsymbol{x}}_i^i+\boldsymbol{B}_i^iu_i(t)+\boldsymbol{G}_i^i[\boldsymbol{y}_i^i(t)-\boldsymbol{C}_i^i\hat{\boldsymbol{x}}_i^i(t)],\\ \boldsymbol{r}_i^i(t)=\boldsymbol{y}_i^i(t)-\boldsymbol{C}_i^i\hat{\boldsymbol{x}}_i^i(t),\end{cases}\tag{22}$$

where $i=1,2,\ldots,N$. $\hat{\boldsymbol{x}}_i^i=[\hat{\xi}_i\ \hat{\zeta}_i]^{\mathrm{T}}\in\mathbb{R}^2$ is the state estimation of the i agent. $\boldsymbol{y}_i^i=[y_i^{\xi}\ y_i^{\zeta}]\in\mathbb{R}^2$ is the output of the ith agent. $\boldsymbol{r}_i^i\in\mathbb{R}^2$ is the residual of the i agent. The vale of $\boldsymbol{A}_i^i$, $\boldsymbol{B}_i^i$, and $\boldsymbol{C}_i^i$ are as follows.

$$\boldsymbol{A}_i^i=\begin{bmatrix}0&1\\0&0\end{bmatrix},\quad \boldsymbol{B}_i^i=\begin{bmatrix}0\\1\end{bmatrix},\quad \boldsymbol{C}_i^i=\begin{bmatrix}1&0\\0&1\end{bmatrix}.$$

It is obvious that the pair $(\boldsymbol{A}_i^i,\boldsymbol{C}_i^i)$ is observable. $\boldsymbol{G}_i^i$ is the parameter to be designed and satisfies that $\boldsymbol{A}_i^i-\boldsymbol{G}_i^i\boldsymbol{C}_i^i$ is stable.

It can be seen from (22) that if there is no fault occurring in the ith agent, $\|\boldsymbol{r}_i^i(t)\|$ approaches to zero asymptotically. Otherwise, $\|\boldsymbol{r}_i^i(t)\|$ approaches to a non-zero constant asymptotically.

Define $J_i^k(t)=\|\boldsymbol{r}_i^k(t)\|$ and $J_{i,\mathrm{th}}^k\in\mathbb{R}$ as the fault isolation evaluation function and the fault isolation threshold of the ith agent for the kth agent, respectively, where $i=1,2,\ldots,N$ and $k\in\bar{\mathcal{N}}_i$. After a fault is detected, according to (12) and (22), the fault isolation logic in the ith agent is designed as Algorithm 2.

Algorithm 2 Fault isolation logic of the ith agent

if $J_i^i(t)\geqslant J_{i,\mathrm{th}}^i$ **then**
  The ith agent is faulty.
else if $\exists k\in\mathcal{N}_i$, $\forall p\in\mathcal{N}_i\backslash\{k\}$, $[J_i^k(t)<J_{i,\mathrm{th}}^k]\wedge[J_i^p(t)\geqslant J_{i,\mathrm{th}}^p]$ **then**
  The kth agent is faulty.
else if $\forall k\in\mathcal{N}_i$, $J_i^k(t)\geqslant J_{i,\mathrm{th}}^k$ **then**
  The faulty agent belongs to $\mathcal{V}\backslash\bar{\mathcal{N}}_i$.
end if

Remark 8. In Algorithm 2, the relationship of sensitivity (or robustness) between residuals and faults is used to isolate faults in neighbors. More concretely, for agent i, if there exists an residual $\boldsymbol{r}_i^k$, $k\in\mathcal{N}_i$, such that the evaluation function of $\boldsymbol{r}_i^k$ is less than its corresponding threshold and the evaluation functions of all the other residuals $\boldsymbol{r}_i^p$, $p\in\mathcal{N}_i\setminus\{k\}$, are all larger than or equal to their corresponding thresholds, then it can be identified that a fault occurs in the kth agent.

Remark 9. The value of $J_{i,\mathrm{th}}^k$, $k\in\bar{\mathcal{N}}_i$, can be determined according to the fault isolation rates, uncertainties, disturbances, and noises of the system. The detailed design of the fault isolation thresholds can also be found in [34, 35].

4 Experimental results

In this section, an experiment is conducted based on a formation platform consisting of three quadrotors, which is described in Figure 2. In the experiment, the communication topology of three quadrotors

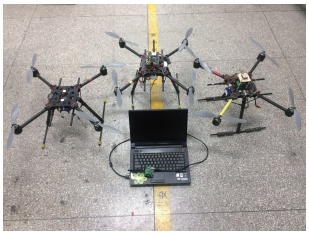

Figure 2 (Color online) The picture of the formation platform.

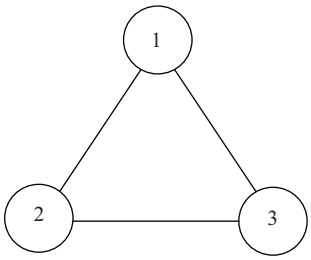

Figure 3 The communication topology of quadrotors.

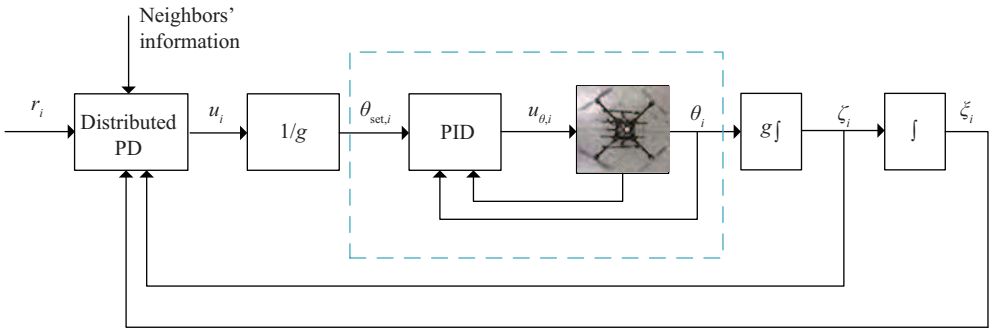

Figure 4 (Color online) The control framework of a quadrotor along x axis.

is set as Figure 3. The Laplacian matrix of the communication topology of three quadrotors is $\boldsymbol{L}_g = [2, -1, -1; -1, 2, -1; -1, -1, 2]$. The eigenvalues of $\boldsymbol{L}_g$ are $\lambda_1 = 0$, $\lambda_2 = \lambda_3 = 3$.

According to [37], the dynamic model of a quadrotor can be regarded as linear and is decoupled along x, y, and z axes when the quadrotor flyes in a hovering state and the rotation angles of the quadrotor are small. Therefore, the control law and the fault diagnosis scheme for a quadrotor can be designed along x, y, and z axes, respectively. In the experiment, we mainly consider distributed fault diagnosis for quadrotors along x axis. The dynamic of a quadrotor along x is $\ddot{\xi}_i(t) = \theta_i(t)g$ and $J_x\ddot{\theta}_i(t) = u_{\theta,i}(t)$, where $i = 1, 2, 3$. $\xi_i \in \mathbb{R}$ is the position of the ith quadrotor along x axis. $\theta_i \in \mathbb{R}$ is the pitch angle of the ith quadrotor. $u_{\theta,i} \in \mathbb{R}$ is the input of the ith quadrotor. $J_x \in \mathbb{R}$ is the rotation inertial of quadrotors and $g \in \mathbb{R}$ is the gravity accelerator.

In the experiment, the control law of each quadrotor consists of two controllers, namely, the internal-loop proportion-integration-derivation controller and the external DPD controller. The control frame of the ith quadrotor along x axis is as Figure 4. In Figure 4, $\zeta_i \in \mathbb{R}$ is the velocity of the ith quadrotor along x axis. $\theta_{\text{set},i}$ is the given pitch angle of the ith quadrotor. According to [38], the dynamic model from $\theta_{\text{set},i}$ to θ_i can be regarded as the proportion one. Therefore, the dynamic from u_i to ξ_i can be considered as a second-order integrator, which can be described as $\dot{\xi}_i(t) = \zeta_i(t)$ and $\dot{\zeta}_i(t) = u_i(t)$.

In the experiment, three quadrotors are set to maintain a triangle and move along x axis in the $x-O-y$ plane with a constant height. The given trajectory along x axis of the system is $r(t) = 43.5 - 0.5t(m)$. Then it follows that $\dot{r}(t) = -0.5(m/s)$, $\ddot{r}(t) = 0(m/s^2)$. The formation vector is $\boldsymbol{d} = [0, \ -5m, \ -5m]^{\mathrm{T}}$. The control parameters in the experiment are $k_1 = 3$, $k_2 = 0.17$, $k_3 = 3$, and $k_4 = 0.37$. It is obvious that $k_1 - k_2\lambda_2 = 2.49 > 0$ and $k_3^2 - 2k_1 - k_4^2\lambda_2^2 = 7.4279 > 0$ hold, which means that the formation can be achieved with any finite time delays.

In the experiment, the time delay is implemented in a software way, which means that the neighboring data used in the distributed control law and the distributed fault diagnosis scheme are delayed in the micro-processors of quadrotors to simulate the time delay during the communication. The time delay is set to be $\tau = 1$ s. The total experimental time is 60.9875 s. In the experiment, assume that a sensor fault with amplitude -2 m/s occurs in the first quadrotor at 655.2025 s. Parameters of fault detection residual generators and fault isolation residual generators can be found in Appendix B. The fault detection

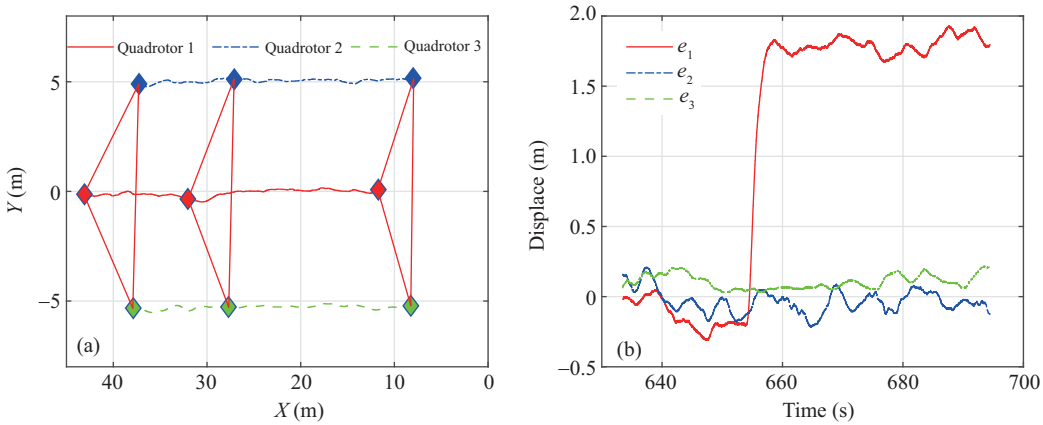

Figure 5 (Color online) The formation results of all quadrotors. (a) The trajectories of three quadrotors; (b) the tracking errors of three quadrotors.

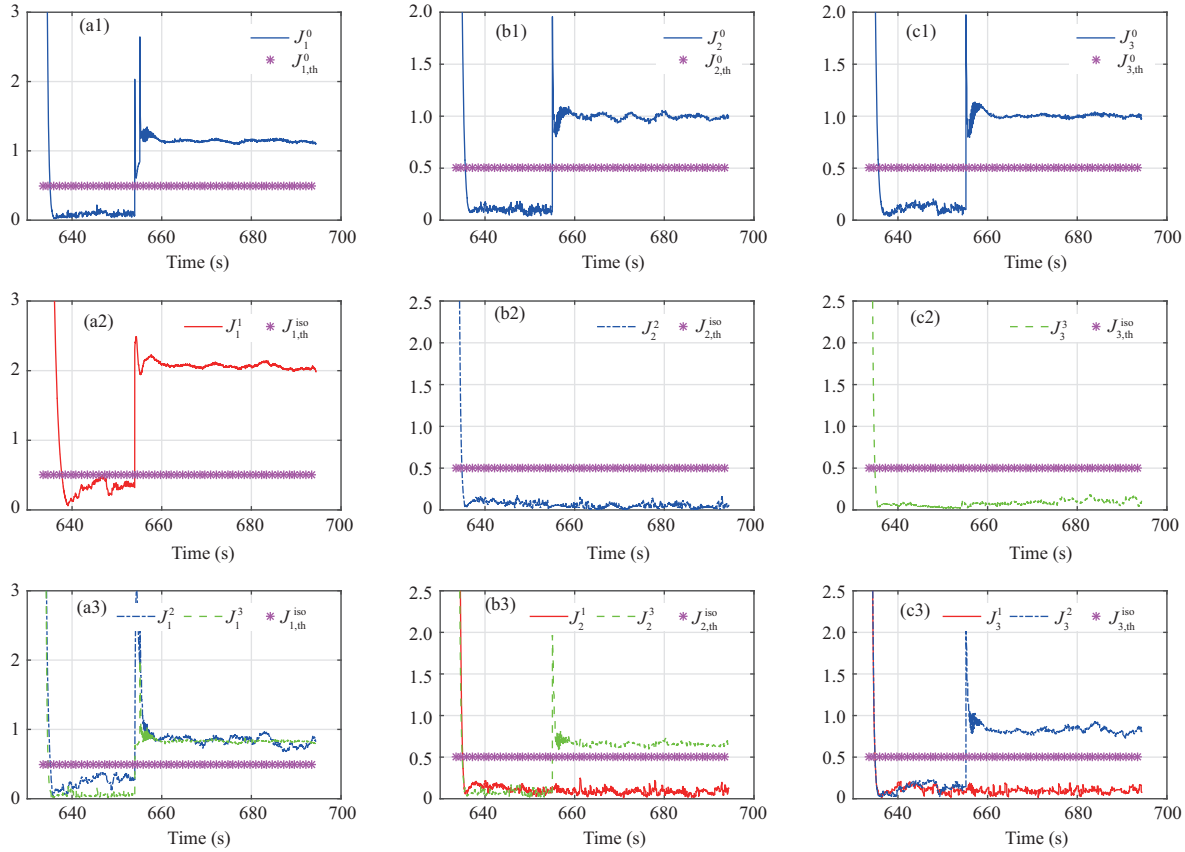

Figure 6 (Color online) The fault diagnosis results of all quadrotors. (a1) The distributed fault detection results in quadrotor 1; (a2) the self-fault detection results in quadrotor 1; (a3) the distributed fault isolation results in quadrotor 1; (b1) the distributed fault detection results in quadrotor 2; (b2) the self-fault detection results in quadrotor 2; (b3) the distributed fault isolation results in quadrotor 2; (c1) the distributed fault detection results in quadrotor 3; (c2) the self-fault detection results in quadrotor 3; (c3) the distributed fault isolation results in quadrotor 3.

threshold of the ith agent is $J^0_{i,\mathrm{th}} = 0.5$, $i = 1, 2, 3$. Fault isolation thresholds are $J^1_{1,\mathrm{th}} = J^2_{1,\mathrm{th}} = J^3_{1,\mathrm{th}} = J^{\mathrm{iso}}_{1,\mathrm{th}} = 0.5$, $J^1_{2,\mathrm{th}} = J^2_{2,\mathrm{th}} = J^3_{2,\mathrm{th}} = J^{\mathrm{iso}}_{2,\mathrm{th}} = 0.5$, and $J^1_{3,\mathrm{th}} = J^2_{3,\mathrm{th}} = J^3_{3,\mathrm{th}} = J^{\mathrm{iso}}_{3,\mathrm{th}} = 0.5$. The formation results of three quadrotors are shown in Figure 5. From Figure 5, the formation stability can be achieved when there is no fault and the formation is damaged after the fault occurs.

The fault detection and fault isolation results are demonstrated in Figures 6. It can be shown from the upper three subgraphs of Figures 6 that the fault can be detected by the all quadrotors according to

Algorithm 1. Moreover, according to the other subgraphs and Algorithm 2, the fault can also be isolated by three quadrotors. The video of the experimental process can be found at the webpages[1)].

5 Conclusion

In the paper, problems of formation control and distributed fault diagnosis for a second-order multi-agent system with unknown constant time delays have been considered. Under an existing DPD control law, the condition on the delay-independent asymptotical formation stability has been presented. Distributed fault detection and isolation schemes have been designed and conditions on the existence of the schemes have been provided. Experimental results have demonstrated the validation of the proposed schemes.

Acknowledgements This work was supported by National Natural Science Foundation of China (Grant Nos. 61210012, 61490701, 61522309, 61473163), Tsinghua University Initiative Scientific Research Program, and Research Fund for the Taishan Scholar Project of Shandong Province of China.

References

1 Oh K K, Park M C, Ahn H S. A survey of multi-agent formation control. Automatica, 2015, 53: 424–440
2 Olfati-Saber R, Fax J A, Murray R M. Consensus and cooperation in networked multi-agent systems. Proc IEEE, 2007, 95: 215–233
3 Ren W, Atkins E. Distributed multi-vehicle coordinated controlvia local information exchange. Int J Robust Nonlin Control, 2007, 17: 1002–1033
4 Chen J, Gan M G, Huang J, et al. Formation control of multiple Euler-Lagrange systems via null-space-based behavioral control. Sci China Inf Sci, 2016, 59: 010202
5 Zhao D Y, Zhao Y R, Cui B H, et al. Sychronized control for mechanical systems. J Shandong Univ Sci Technol, 2013, 32: 1–6
6 Fax J A, Murray R M. Information flow and cooperative control of vehicle formations. IEEE Trans Automat Contr, 2004, 49: 1465–1476
7 Wang W, Huang J S, Wen C Y, et al. Distributed adaptive control for consensus tracking with application to formation control of nonholonomic mobile robots. Automatica, 2014, 50: 1254–1263
8 Zhao G, Zhao D Y, Zhao Y R, et al. Leader-follower based distributed synchronous control and simulation for multi-manipulators system. J Shandong Univ Sci Technol, 2014, 33: 99–104
9 Campa G, Gu Y, Seanor B, et al. Design and flight-testing of non-linear formation control laws. Control Eng Practice, 2007, 15: 1077–1092
10 Shen D B, Sun Z D, Sun W J. Leader-follower formation control without leader's velocity information. Sci China Inf Sci, 2014, 57: 092202
11 Nagy M, Ákos Z, Biro D, et al. Hierarchical group dynamics in pigeon flocks. Nature, 2010, 464: 890–893
12 Kozyreff G, Vladimirov A G, Mandel P. Global coupling with time delay in an array of semiconductor lasers. Phys Rev Lett, 2000, 85: 3809–3812
13 Lin P, Jia Y M, Li L. Distributed robust consensus control in directed networks of agents with time-delay. Syst Control Lett, 2008, 57: 643–653
14 Papachristodoulou A, Jadbabaie A, Münz U. Effects of delay in multi-agent consensus and oscillator synchronization. IEEE Trans Automat Contr, 2010, 55: 1471–1477
15 Abdessameud A, Tayebi A. Formation control of VTOL unmanned aerial vehicles with communication delays. Automatica, 2011, 47: 2383–2394
16 Olfati-Saber R, Murray R M. Consensus problems in networks of agents with switching topology and time-delays. IEEE Trans Automat Contr, 2004, 49: 1520–1533
17 Tian Y P, Liu C L. Consensus of multi-agent systems with diverse input and communication delays. IEEE Trans Automat Contr, 2008, 53: 2122–2128
18 Münz U, Papachristodoulou A, Allgöwer F. Delay robustness in consensus problems. Automatica, 2010, 46: 1252–1265
19 Xu J J, Zhang H S, Xie L H. Input delay margin for consensusability of multi-agent systems. Automatica, 2013, 49: 1816–1820
20 Dong X W, Yu B C, Shi Z Y, et al. Time-varying formation control for unmanned aerial vehicles: theories and applications. IEEE Trans Contr Syst Technol, 2015, 23: 340–348
21 Daigle M J, Koutsoukos X D, Biswas G. Distributed diagnosis in formations of mobile robots. IEEE Trans Robot, 2007, 23: 353–369
22 Qin L G, He X, Zhou D H. A survey of fault diagnosis for swarm systems. Syst Sci Control Eng, 2014, 2: 13–23
23 Micalizio R, Torasso P, Torta G. On-line monitoring and diagnosis of a team of service robots: a model-based approach. AI Commun, 2006, 19: 313–340

1) https://youtu.be/pFepIOQPLeE or http://v.youku.com/v_show/id_XMjQ5NzYzMDA5Ng==.html.

24 Léchevin N, Rabbath C A. Decentralized detection of a class of non-abrupt faults with application to formations of unmanned airships. IEEE Trans Contr Syst Technol, 2009, 17: 484–493
25 Zhang K, Jiang B, Shi P. Adjustable parameter-based distributed fault estimation observer design for multiagent systems with directed graphs. IEEE Trans Cybern, 2017, 47: 306–314
26 Meskin N, Khorasani K. Actuator fault detection and isolation for a network of unmanned vehicles. IEEE Trans Automat Contr, 2009, 54: 835–840
27 Davoodi M R, Khorasani K, Talebi H A, et al. Distributed fault detection and isolation filter design for a network of heterogeneous multiagent systems. IEEE Trans Contr Syst Technol, 2014, 22: 1061–1069
28 Arrichiello F, Marino A, Pierri F. Observer-based decentralized fault detection and isolation strategy for networked multirobot systems. IEEE Trans Contr Syst Technol, 2015, 23: 1465–1476
29 Shames I, Teixeira A M, Sandberg H, et al. Distributed fault detection for interconnected second-order systems. Automatica, 2011, 47: 2757–2764
30 Teixeira A, Shames I, Sandberg H, et al. Distributed fault detection and isolation resilient to network model uncertainties.. IEEE Trans Cybern, 2014, 44: 2024–2037
31 Shi J T, He X, Wang Z D, et al. Distributed fault detection for a class of second-order multi-agent systems: an optimal robust observer approach. IET Contr Theor Appl, 2014, 8: 1032–1044
32 Gao X W, Liu X H, Han J. Reduced order unknown input observer based distributed fault detection for multi-agent systems. J Franklin Institute, 2017, 354: 1464–1483
33 Qin L G, He X, Zhou D H. Distributed proportion-integration-derivation formation control for second-order multi-agent systems with communication time delays. Neurocomputing, 2017, 267: 271–282
34 Chen J, Patton R J. Robust Model-Based Fault Diagnosis for Dynamic. New York: Springer Science & Business Media, 1999. 51–54
35 Ding S X. Model-Based Fault Diagnosis Techniques: Design Schemes, Algorithms, and Tools. London: Springer-Verlag, 2008. 286–312
36 Hou M, Muller P C. Design of observers for linear systems with unknown inputs. IEEE Trans Automat Contr, 1992, 37: 871–875
37 Zhang Y M, Chamseddine A, Rabbath C A, et al. Development of advanced FDD and FTC techniques with application to an unmanned quadrotor helicopter testbed. J Franklin Institute, 2013, 350: 2396–2422
38 Qin L G, He X, Yan R, et al. Active fault-tolerant control for a quadrotor with sensor faults. J Intell Robot Syst, 2017, 88: 449–467

Appendix A Proof of Lemma 1

Proof. The dynamic of the tracking error of the ith agent can be described as

$$\ddot{e}_i(t) = -k_1 e_i(t) - k_2 \sum_{j\in\mathcal{N}_i} a_{ij}[e_i(t-\tau) - e_j(t-\tau)] - k_3\dot{e}_i(t) - k_4 \sum_{j\in\mathcal{N}_i} a_{ij}[\dot{e}_i(t-\tau) - \dot{e}_j(t-\tau)],$$

where $i = 1, 2, \ldots, N$. It is also assumed that $r(t-\tau) = 0$ and $\dot{r}(t-\tau) = 0$ when $t \leqslant \tau$.

Let $\boldsymbol{e}(t) = [e_1(t), \ldots, e_N(t), \dot{e}_1(t), \ldots, \dot{e}_N(t)]^{\mathrm{T}}$. It follows that $\dot{\boldsymbol{e}}(t) = \boldsymbol{A}_1\boldsymbol{e}(t) + \boldsymbol{A}_2\boldsymbol{e}(t-\tau)$ holds, where

$$\boldsymbol{A}_1 = \begin{bmatrix} \boldsymbol{0} & \boldsymbol{I}_N \\ -k_1\boldsymbol{I}_N & -k_3\boldsymbol{I}_N \end{bmatrix} = \begin{bmatrix} 0 & 1 \\ -k_1 & -k_3 \end{bmatrix} \otimes \boldsymbol{I}_N,\ \boldsymbol{A}_2 = \begin{bmatrix} \boldsymbol{0} & \boldsymbol{0} \\ -k_2\boldsymbol{L}_g & -k_4\boldsymbol{L}_g \end{bmatrix} = \begin{bmatrix} 0 & 0 \\ -k_2 & -k_4 \end{bmatrix} \otimes \boldsymbol{L}_g.$$

Because $\boldsymbol{L}_g$ is an Hermitian matrix, there exists an orthogonal matrix $\boldsymbol{U}$ such that $\boldsymbol{U}^{\mathrm{T}}\boldsymbol{L}_g\boldsymbol{U} = \mathrm{diag}\{\lambda_1, \ldots, \lambda_N\}$. Let $\boldsymbol{T}_1 = \boldsymbol{I}_2 \otimes \boldsymbol{U}^{\mathrm{T}}$ and $\boldsymbol{T}_2 = [\boldsymbol{i}_1, \boldsymbol{i}_{N+1}, \boldsymbol{i}_2, \boldsymbol{i}_{N+2}, \ldots, \boldsymbol{i}_N, \boldsymbol{i}_{2N}]^{\mathrm{T}}$, where $\boldsymbol{i}_k$ is the kth column of the matrix $\boldsymbol{I}_{2N}$. It follows that

$$\tilde{\boldsymbol{A}}_1 = \boldsymbol{T}_2\boldsymbol{T}_1\boldsymbol{A}_1\boldsymbol{T}_1^{-1}\boldsymbol{T}_2^{-1} = \boldsymbol{I}_N \otimes \begin{bmatrix} 0 & 1 \\ -k_1 & -k_3 \end{bmatrix},\ \tilde{\boldsymbol{A}}_2 = \boldsymbol{T}_2\boldsymbol{T}_1\boldsymbol{A}_2\boldsymbol{T}_1^{-1}\boldsymbol{T}_2^{-1} = \mathrm{diag}\{\lambda_1, \ldots, \lambda_N\} \otimes \begin{bmatrix} 0 & 0 \\ -k_2 & -k_4 \end{bmatrix}.$$

Let $\tilde{\boldsymbol{e}} = \boldsymbol{T}_2\boldsymbol{T}_1\boldsymbol{e}$. It can be derived that $\dot{\tilde{\boldsymbol{e}}}(t) = \tilde{\boldsymbol{A}}_1\tilde{\boldsymbol{e}}(t) + \tilde{\boldsymbol{A}}_2\tilde{\boldsymbol{e}}(t-\tau)$. Furthermore, it follows that

$$\dot{\boldsymbol{\eta}}_i(t) = \begin{bmatrix} 0 & 1 \\ -k_1 & -k_3 \end{bmatrix} \boldsymbol{\eta}_i(t) + \lambda_i \begin{bmatrix} 0 & 0 \\ -k_2 & -k_4 \end{bmatrix} \boldsymbol{\eta}_i(t-\tau), \tag{A1}$$

where $i = 1, 2, \ldots, N$. $\boldsymbol{\eta}_i \in \mathbb{R}^2$ consists of the $(2i-1)$th and $(2i)$th elements of $\tilde{\boldsymbol{e}}$.

The characteristic equation of the system (A1) is $s^2 + k_3 s + k_1 + (k_4 s + k_2)\lambda_i \mathrm{e}^{-\tau s} = 0$. If all roots of the above equation lie in the left half complex plane, the system (A1) is stable. Define a function $G_i(s)$ as follows.

$$G_i(s) = \frac{(k_4 s + k_2)\lambda_i \mathrm{e}^{-\tau s}}{s^2 + k_3 s + k_1},\quad i = 1, 2, \ldots, N. \tag{A2}$$

Let $s = \mathrm{j}w$, where $\mathrm{j}^2 = -1$ and $w \in \mathbb{R}$. It follows that

$$G_i(\mathrm{j}w) = \frac{(k_2 + \mathrm{j}wk_4)\lambda_i \mathrm{e}^{-\mathrm{j}w\tau}}{k_1 - w^2 + \mathrm{j}k_3 w},\quad i = 1, 2, \ldots, N. \tag{A3}$$

Since $k_1 > 0$ and $k_2 > 0$, it follows that all roots of the equation $s^2 + k_3 s + k_1 = 0$ lie in the left half complex plane. According to the Nyquist stability criterion and the literature [2)3)], the number of the roots of $s^2 + k_3 s + k_1 + (k_4 s + k_2)\lambda_i \mathrm{e}^{-\tau s} = 0$ with positive real part is equal to the number of the times for which the Nyquist curve of $G_i(\mathrm{j}w)$ encloses the point $(-1, 0)$ as the w increases from 0 to ∞. Therefore, the condition on the asymptotical formation stability can be gained by analyzing the characteristic of the Nyquist curve of $G_i(\mathrm{j}w)$.

According to (A3), the amplitude of $G_i(\mathrm{j}w)$ is

$$|G_i(\mathrm{j}w)| = \frac{\lambda_i \sqrt{k_2^2 + (wk_4)^2}}{\sqrt{(k_1 - w^2)^2 + (wk_3)^2}}, \quad i = 1, 2, \ldots, N. \tag{A4}$$

When $i = 1$, it follows that $\lambda_i = 0$ and $|G_i(\mathrm{j}w)| = 0$. It is obvious that the Nyquist curve of $G_1(\mathrm{j}w)$ dose not enclose the point $(-1, 0)$ and the system (A1) is stable when $i = 1$. When $i \in \{2, 3, \ldots, N\}$, since $k_1 > k_2 \lambda_N$, it follows that $k_1 > k_2 \lambda_i$ holds. Since $k_3^2 - 2k_1 - k_4^2 \lambda_N^2 > 0$, it is obvious that $k_3^2 - 2k_1 - k_4^2 \lambda_i^2 > 0$ holds, where $i = 2, 3, \ldots, N$. Then, the following equation can be obtained.

$$w^4 + (k_3^2 - 2k_1 - k_4^2 \lambda_i^2) w^2 + k_1^2 - k_2^2 \lambda_i^2 > 0, \quad i = 2, 3, \ldots, N. \tag{A5}$$

According to (A4) and (A5), it can be obtained that $|G_i(\mathrm{j}w)| < 1$ holds, where $i = 2, 3, \ldots, N$. Hence, the Nyquist curve of $G_i(\mathrm{j}w)$ dose not enclose the point $(-1, 0)$, $i = 1, 2, \ldots, N$. The system (A1) is stable when $i = 2, 3, \ldots, N$. Overall, the formation system is stable and the asymptotical formation stability is achieved. This ends the proof.

Appendix B Parameters in the experiment

$$\boldsymbol{G}_1^0 = \begin{bmatrix} 3 & 0 & 0 & 1 & 0 & 0 \\ 6 & 6 & 0 & 1 & 1 & 0 \\ 9 & 0 & 9 & 1 & 0 & 1 \\ -3 & 0.17 & 0.17 & 9 & 0.37 & 0.37 \\ -3 & -3.34 & 0.17 & 12 & 11.26 & 0.37 \\ -3 & 0.17 & -3.34 & 15 & 0.37 & 14.26 \end{bmatrix}, \boldsymbol{G}_2^0 = \begin{bmatrix} 2 & 2 & 0 & 1 & 1 & 00 \\ 4 & 0 & 0 & 1 & 0 & 0 \\ 6 & 0 & 6 & 1 & 0 & 1 \\ -3 & -3.34 & 0.17 & 5 & 4.26 & 0.37 \\ -3 & 0.17 & 0.17 & 7 & 0.37 & 0.37 \\ -3 & 0.17 & -3.34 & 9 & 0.37 & 8.26 \end{bmatrix}, \boldsymbol{G}_3^0 = \begin{bmatrix} 2 & 2 & 0 & 1 & 1 & 0 \\ 4 & 0 & 4 & 1 & 0 & 1 \\ 6 & 0 & 0 & 1 & 0 & 0 \\ -3 & -3.34 & 0.17 & 5 & 4.26 & 0.37 \\ -3 & 0.17 & -3.34 & 7 & 0.37 & 6.26 \\ -3 & 0.17 & 0.17 & 9 & 0.37 & 0.37 \end{bmatrix},$$

$$\boldsymbol{H}_1^2 = \begin{bmatrix} 0 & 0 & 1 & 0 & 0 & 0 \\ 0 & -1 & 0 & 0 & 0 & 0 \\ -1 & 0 & 0 & 0 & 0 & 0 \\ 0 & 0 & 0 & 0 & 0 & 1 \end{bmatrix}, \boldsymbol{F}_1^2 = \begin{bmatrix} -10.0047 & -0.0000 & 4.4964 & 0.5801 & 5.6948 \\ 0.0000 & -10.0000 & 0 & -0.0000 & 0.0000 \\ -1.6615 & -0.0000 & -2.3022 & 0.3298 & 2.2370 \\ -0.3855 & -0.0000 & 0.4673 & -5.9239 & 0.7048 \\ -1.4658 & -0.0000 & 1.6772 & 0.4651 & -1.7692 \end{bmatrix}, \boldsymbol{M}_1^2 = \begin{bmatrix} 0 & 0 & 0 \\ 0 & 0 & 0 \\ 0.9904 & 0.0970 & -0.0096 \\ 0.0970 & 0.0192 & 0.0970 \\ -0.0096 & 0.0970 & 0.9904 \end{bmatrix},$$

$$\boldsymbol{S}_1^2 = \begin{bmatrix} 10.4287 & 10.0047 & 0.0000 & -10.1081 & 0 & -5.6533 \\ 10.0000 & -0.0000 & 10.0000 & 1.0000 & 0 & 1.0000 \\ -1.9049 & 1.5042 & 0.2169 & -3.3315 & 0 & -1.8314 \\ 5.7273 & 0.3544 & -0.3043 & 0.3506 & 0 & -0.4386 \\ -2.2373 & 1.3084 & -3.2931 & -3.3315 & 0 & -1.9486 \end{bmatrix}, \boldsymbol{J}_1^2 = \begin{bmatrix} 0 & -1.0000 & -0.0980 & 0.9904 & -0.0980 \\ 1.0000 & 0 & 0.0980 & -0.9904 & 0.0980 \\ 0 & 0 & -0.0980 & 0.9904 & -0.0980 \\ 0 & 0 & 1.0000 & -0.0000 & -1.0000 \end{bmatrix},$$

$$\boldsymbol{F}_1^3 = \begin{bmatrix} -16.0002 & -0.0260 & 0.0000 & -0.0000 & 0.0000 \\ -0.3347 & -31.9998 & 5.0541 & 5.0541 & 1.0000 \\ -0.5072 & -23.2880 & -4.0763 & 3.9144 & 0.8184 \\ -0.5072 & -23.2880 & 3.9144 & -3.9096 & -0.0242 \\ -0.1004 & -4.6078 & 0.8184 & -0.0242 & -4.0141 \end{bmatrix}, \boldsymbol{M}_1^3 = \begin{bmatrix} 0 & 0 & 0 \\ 0 & 0 & 0 \\ 0.9904 & -0.0096 & 0.0970 \\ -0.0096 & 0.9904 & 0.0970 \\ 0.0970 & 0.0970 & 0.0192 \end{bmatrix},$$

$$\boldsymbol{H}_1^3 = \begin{bmatrix} 0 & 0 & 1 & 0 & 0 & 0 \\ 0 & -1 & 0 & 0 & 0 & 0 \\ 0 & 0 & 0 & 0 & 1 & 0 \\ -1 & 0 & 0 & 0 & 0 & 0 \end{bmatrix}, \boldsymbol{S}_1^3 = \begin{bmatrix} 16.0262 & 16.0002 & 0.0260 & 1.0000 & 1.0000 & 0 \\ 32.3345 & 0.3347 & 31.9998 & -10.1081 & -5.0541 & 0 \\ 19.7353 & 0.7241 & 23.1306 & -3.3315 & -3.5571 & 0 \\ 20.5861 & -2.7859 & 23.1306 & -3.3315 & 0.2402 & 0 \\ 8.1215 & -0.2040 & 4.5767 & 0.3506 & 0.1014 & 0 \end{bmatrix},$$

$$\boldsymbol{J}_1^3 = \begin{bmatrix} 0 & -1.0000 & -0.0980 & -0.0980 & 0.9904 \\ 1.0000 & 0 & 0.0980 & 0.0980 & -0.9904 \\ 0 & 0 & 1.0000 & -1.0000 & -0.0000 \\ 0 & 0 & -0.0980 & -0.0980 & 0.9904 \end{bmatrix},$$

$$\boldsymbol{F}_2^1 = \begin{bmatrix} -3.0000 & 0.0000 & 0.0000 & -0.0000 & -0.0000 \\ -0.0000 & -15.0000 & -0.0000 & 0.0000 & 0.0000 \\ 0.0000 & -0.0000 & -21.6599 & 7.2461 & 7.2461 \\ 0.0000 & -0.0000 & -8.4386 & -2.6700 & 3.3300 \\ 0.0000 & -0.0000 & -8.4386 & 3.3300 & -2.6700 \end{bmatrix}, \boldsymbol{S}_2^1 = \begin{bmatrix} 3.0000 & -0.0000 & -0.0000 & 1.0000 & 0 & -0.0000 \\ 15.0000 & 0.0000 & 15.0000 & 1.0000 & 0 & 1.0000 \\ 22.2311 & 22.8398 & -0.3043 & -10.6504 & 0 & -5.3252 \\ 5.1884 & 8.2645 & 0.2169 & -2.2431 & 0 & -2.0666 \\ 5.1884 & 8.2645 & -3.2931 & -2.2431 & 0 & -0.1766 \end{bmatrix}, \boldsymbol{H}_2^1 = \begin{bmatrix} 0 & 0 & 1 & 0 & 0 & 0 \\ 0 & -1 & 0 & 0 & 0 & 0 \\ -1 & 0 & 0 & 0 & 0 & 0 \\ 0 & 0 & 0 & 0 & 0 & 1 \end{bmatrix},$$

$$\boldsymbol{M}_2^1 = \begin{bmatrix} 0 & 0 & 0 \\ 0 & 0 & 0 \\ 0.0192 & 0.0970 & 0.0970 \\ 0.0970 & 0.9904 & -0.0096 \\ 0.0970 & -0.0096 & 0.9904 \end{bmatrix}, \boldsymbol{J}_2^1 = \begin{bmatrix} 1.0000 & -1.0000 & 0 & 0 & 0 \\ -1.0000 & 0 & 0.9904 & -0.0980 & -0.0980 \\ 1.0000 & 0 & 0 & 0 & 0 \\ 0 & 0 & -0.0000 & 1.0000 & -1.0000 \end{bmatrix}, \boldsymbol{F}_2^3 = \begin{bmatrix} -12.0000 & 0.0110 & -0.0000 & -0.0000 & 0.0000 \\ 0.1622 & -24.0000 & 5.0541 & 5.0541 & 1.0000 \\ 0.1868 & -13.0993 & -3.0576 & 2.9419 & 0.5849 \\ 0.1868 & -13.0993 & 2.9419 & -2.9435 & 0.0085 \\ 0.0370 & -2.5918 & 0.5849 & 0.0085 & -2.9989 \end{bmatrix},$$

$$\boldsymbol{M}_2^3 = \begin{bmatrix} 0 & 0 & 0 \\ 0 & 0 & 0 \\ 0.9904 & -0.0096 & 0.0970 \\ -0.0096 & 0.9904 & 0.0970 \\ 0.0970 & 0.0970 & 0.0192 \end{bmatrix}, \boldsymbol{H}_2^3 = \begin{bmatrix} 0 & 0 & 1 & 0 & 0 & 0 \\ 0 & -1 & 0 & 0 & 0 & 0 \\ 0 & 0 & 0 & 0 & 1 & 0 \\ -1 & 0 & 0 & 0 & 0 & 0 \end{bmatrix}, \boldsymbol{S}_2^3 = \begin{bmatrix} 11.9890 & -0.0000 & -0.0110 & 1.0000 & 0.0000 & 0 \\ 23.8378 & 0.0000 & 24.0000 & -10.1081 & -5.0541 & 0 \\ 9.0884 & -3.8837 & 12.9420 & -3.3315 & -0.7700 & 0 \\ 9.6705 & 0.2084 & 12.9420 & -3.3315 & -2.6024 & 0 \\ 4.9432 & 2.7238 & 2.5607 & 0.3506 & 0.3822 & 0 \end{bmatrix},$$

2) Ansoff H, Krumhansl J. A general stability criterion for linear oscillating systems with constant time lag. Quart Appl Math, 1948, 6: 337–341.

3) Ansoff H. Stability of linear oscillating systems with constant time lag. J Appl Mech-Trans ASME, 1949, 16: 158–164.

$$\boldsymbol{J}_2^3 = \begin{bmatrix} 1.0000 & -1.0000 & 0 & 0 & 0 \\ -1.0000 & 0 & -0.0980 & -0.0980 & 0.9904 \\ 0 & 0 & -1.0000 & 1.0000 & 0.0000 \\ 1.0000 & 0 & 0 & 0 & 0 \end{bmatrix}, \boldsymbol{F}_3^1 = \begin{bmatrix} -3.0044 & -0.0000 & -0.0000 & -0.0808 & 0.0808 \\ -0.0000 & -15.0000 & -0.0000 & 0.0000 & 0.0000 \\ -0.0000 & -0.0000 & -21.6599 & 7.2461 & 7.2461 \\ -0.0808 & -0.0000 & -8.4386 & -2.6679 & 3.3278 \\ 0.0808 & -0.0000 & -8.4386 & 3.3278 & -2.6679 \end{bmatrix}, \boldsymbol{H}_3^1 = \begin{bmatrix} 0 & 0 & 1 & 0 & 0 & 0 \\ 0 & -1 & 0 & 0 & 0 & 0 \\ -1 & 0 & 0 & 0 & 0 & 0 \\ 0 & 0 & 0 & 0 & 0 & 1 \end{bmatrix},$$

$$\boldsymbol{M}_3^1 = \begin{bmatrix} 0 & 0 & 0 \\ 0 & 0 & 0 \\ 0.0192 & 0.0970 & 0.0970 \\ 0.0970 & 0.9904 & -0.0096 \\ 0.0970 & -0.0096 & 0.9904 \end{bmatrix}, \boldsymbol{S}_3^1 = \begin{bmatrix} 3.0044 & 0.0000 & 3.0044 & 1.0000 & 01.0808 \\ 15.0000 & 0.0000 & 0.0000 & 1.0000 & 0-0.0000 \\ 22.2311 & 22.8398 & -0.3043 & -10.6504 & 0-5.3252 \\ 5.2692 & 8.2645 & -3.2122 & -2.2431 & 0-0.1788 \\ 5.1075 & 8.2645 & 0.1361 & -2.2431 & 0-2.0644 \end{bmatrix}, \boldsymbol{J}_3^1 = \begin{bmatrix} -1.0000 & 1.0000 & 0 & 0 & 0 \\ 0 & -1.0000 & 0.9904 & -0.0980 & -0.0980 \\ 0 & 1.0000 & 0 & 0 & 0 \\ 0 & 0 & 0.0000 & -1.0000 & 1.0000 \end{bmatrix},$$

$$\boldsymbol{F}_3^2 = \begin{bmatrix} -21.0000 & -0.0000 & 5.0541 & 1.0000 & 5.0541 \\ -0.0000 & -15.0000 & 0.0000 & -0.0000 & -0.0000 \\ -10.4794 & -0.0000 & -2.8595 & -0.1612 & 2.8913 \\ -2.0735 & -0.0000 & -0.1612 & -3.0961 & 0.7738 \\ -10.4794 & -0.0000 & 2.8913 & 0.7738 & -3.0444 \end{bmatrix}, \boldsymbol{M}_3^2 = \begin{bmatrix} 0 & 0 & 0 \\ 0 & 0 & 0 \\ 0.9904 & 0.0970 & -0.0096 \\ 0.0970 & 0.0192 & 0.0970 \\ -0.0096 & 0.0970 & 0.9904 \end{bmatrix}, \boldsymbol{H}_3^2 = \begin{bmatrix} 0 & 0 & 1 & 0 & 0 & 0 \\ 0 & -1 & 0 & 0 & 0 & 0 \\ 0 & 0 & 0 & 0 & 1 & 0 \\ -1 & 0 & 0 & 0 & 0 & 0 \end{bmatrix},$$

$$\boldsymbol{S}_3^2 = \begin{bmatrix} 21.0000 & -0.0000 & 21.0000 & -10.1081 & -5.0541 & 0 \\ 15.0000 & 0.0000 & 0.0000 & 1.0000 & -0.00007 & 0 \\ 7.4086 & -3.1304 & 10.3220 & -3.3315 & -0.8943 & 0 \\ 4.5599 & 2.8219 & 2.0423 & 0.3506 & 1.1379 & 0 \\ 6.4646 & -0.5644 & 10.3220 & -3.3315 & -2.6276 & 0 \end{bmatrix}, \boldsymbol{J}_3^2 = \begin{bmatrix} -1.0000 & 1.0000 & 0 & 0 & 0 \\ 0 & -1.0000 & -0.0980 & 0.9904 & -0.0980 \\ 0 & 0 & -1.0000 & 0.0000 & 1.0000 \\ 0 & 1.0000 & 0 & 0 & 0 \end{bmatrix}.$$